Metal Imidazolato Complexes: Synthesis, Characterization, and X-ray Powder Diffraction Studies of Group 10 Coordination Polymers

Norberto Masciocchi,*,†,‡ G. Attilio Ardizzoia,*,‡,§ Girolamo LaMonica,‡,§ Angelo Maspero,‡,§ Simona Galli,† and Angelo Sironi†

Dipartimento di Chimica Strutturale e Stereochimica Inorganica e Centro CNR, Università di Milano, Via Venezian 21, 20133 Milano, Italy, and Dipartimento di Chimica Inorganica, Metallorganica ed Analitica e Centro CNR, Università di Milano, Via Venezian 21, 20133 Milano, Italy

Received June 4, 2001

Binary metal imidazolates of the group 10 metals have been prepared and typically found amorphous. However, the intermediacy of a number of (poly)crystalline species during their formation has been evidenced; their selective preparation and characterization, by chemical, spectroscopic, and thermal methods and their structure solution by the ab initio X-ray powder diffraction technique lead to the discovery of new interesting structural features, such as those of polymeric $Ni(Him)_2(im)(CH_3COO)$ (Him = imidazole) and of the hydrogen-bonded polymers of general $Pd_xPt_{1-x}(Him)_2(im)_2$ formula ($x = 0, 0.5, 1$). The latter are built upon 2D frameworks of (pseudo)square meshes, which, in the pure Pd derivative, form an entangled structure based upon interpenetrating 2D layers, coupled in pairs. The different structures are discussed in terms of different conformations of the new "im−H−im" ligand, which acts as monoanionic exobidentate fragment, similar to im, pyrazolate (pz), "pz−H−pz", and pyrimidin-2-olate.

Introduction

The last years have witnessed a blooming of chemical, spectroscopic, and structural studies on coordination polymers, whose nature may influence future applications in a number of different fields;[1] for example, some polymeric species of this class have been recently proved to possess interesting electrical, electrochemical, magnetic,[2] optical,[3] anticorrosion,[4] or antimicrobial[5] properties. Most known coordination polymers contain transition metal ions within the backbone, which are held together by polydentate ligands.[6] For example, polypyridyls, polyazines, and related ligands have been used to build complex structures, which, depending on their actual topology, may show interesting sorption,[7] catalytic,[8] or magnetic activity.[9] It is possible, however, to prepare coordination polymers not requiring the presence of counterions, if suitable negatively charged ligands (obtained from deprotonated stable polyazaheterocycles) are used.[10] Therefore, a number of pyrazolato and pyrimidinolato homoleptic species have been recently prepared by us and others,[7c,11,12] which showed the extreme versatility of the supramolecular architectures derived therefrom, highlighting the competition between the formation of cyclic oligomeric species and that of extended (1D or even polydimensional) structures. Indeed, we surprisingly discovered a wide variety of polynuclear arrangements, ranging from trimers, tetramers, and hexamers up to polymeric species, which could be *selectively* prepared and isolated.[12]

Although we have already been working with the imidazolate ligand a few years ago,[13] only recently we have tackled a more systematic study on its coordination chemistry, in search for homoleptic species of $M(im)_2$ (im = imidazolate) general formula. We recently reported on the $Cu(im)_2$ species, which was shown to be (at least) pentamorphic,[14] none of the newly

† Dipartimento di Chimica Strutturale e Stereochimica Inorganica e Centro CNR, Università di Milano.

‡ On leave from the Dipartimento di Scienze Chimiche, Fisiche e Matematiche, Università dell'Insubria, via Valleggio 11, 22100 Como, Italy.

§ Dipartimento di Chimica Inorganica, Metallorganica ed Analitica e Centro CNR, Università di Milano.

(1) Day, P.; *J. Chem. Soc., Dalton Trans.* **2000**, 3483.
(2) Gütlich, P.; Carcia, Y.; Goodwin, H. A. *J. Chem. Soc., Dalton Trans.* **2000**, 419.
(3) Mark, J. E.; Allcock, H. R.; West, R. *Inorganic Polymers*; Prentice Hall Inc.: Englewood Cliffs, NJ, 1992. Wisian-Neilson, P., Allcock, H. R., Wynne, K. J., Eds. *Inorganic and Organometallic Polymers II*; ACS Symposium Series 572; American Chemical Society: Washington, DC, 1994.
(4) Richmond, W. N.; Faguy, P. W.; Weibel, S. C. *J. Electroanal. Chem.* **1998**, *448*, 237−244. Gašparac, R.; Stupnišek-Lisac, E. *Corrosion* **1994**, *55*, 1031.
(5) Kidd, H., James, D. R., Eds. *The Agrochemicals Handbook*, 3rd ed.; Royal Society of Chemistry Information Services: Cambridge, U.K., 1991. For recent examples on silver diazolates, see: Nomiya, K.; Tsuda, K.; Sudoj, T.; Oda, M. *J. Inorg. Biochem.* **1997**, *68*, 39. Nomiya, K.; Tsuda, K.; Kasuga, N. C. *J. Chem. Soc., Dalton Trans.* **1998**, 1653. Nomiya, K.; Takahashi, S.; Noguchi, R.; Nemoto, S.; Takayama, T.; Oda, M. *Inorg. Chem.* **2000**, *39*, 3301.
(6) McCleverty, J. A.; Ward, M. D. *Acc. Chem. Res.* **1998**, *31*, 842.
(7) (a) Kondo, M.; Shimamura, M.; Noro, S.; Minakoshi, S.; Asami, A.; Seki, K.; Kitagawa, S. *Chem. Mater.* **2000**, *12*, 1288. (b) Noro, S.; Kitagawa, S.; Kondo, M.; Seki, K. *Angew. Chem., Int. Ed. Engl.* **2000**, *39*, 2082. (c) Tabares, L. C.; Navarro, J. A. R.; Salas, J. M. *J. Am. Chem. Soc.* **2001**, *123*, 383.
(8) Fujita, M.; Kwon, Y. J.; Washizu, S.; Ogura, K. *J. Am. Chem. Soc.* **1994**, *116*, 1151.
(9) Hao, X.; Wei, Y.; Zhang, S. *Chem. Commun.* **2000**, 2271.
(10) For a recent example, see: Rettig, S. J.; Sanchez, V.; Storr, A.; Thompson, R. C.; Trotter, J. *J. Chem. Soc., Dalton Trans.* **2000**, 3931.
(11) Masciocchi, N.; Ardizzoia, G. A.; LaMonica, G.; Maspero, A.; Sironi, A. *Eur. J.Inorg.Chem.* **2000**, 2507.
(12) (a) Masciocchi, N.; Moret, M.; Cairati, P.; Sironi, A.; Ardizzoia, G. A.; LaMonica, G.; Cenini, S. *J. Am. Chem. Soc.* **1994**, *116*, 7668. (b) Masciocchi, N.; Cairati, P.; Sironi, A. *Powder Diffr.* **1998**, *13*, 35. (c) Ardizzoia, G. A.; Cenini, S.; LaMonica, G.; Masciocchi, N.; Maspero, A.; Moret, M. *Inorg. Chem.* **1998**, *37*, 4284.
(13) Masciocchi, N.; Moret, M.; Cairati, P.; Sironi, A.; Ardizzoia, G. A.; La Monica, G. *J. Chem. Soc., Dalton Trans.* **1995**, 1671.
(14) Masciocchi, N.; Bruni, S.; Cariati, E.; Cariati, F.; Galli, S.; Sironi, A. *Inorg. Chem.* **2001**, *40*, 5897.

10.1021/ic010585d CCC: $20.00
Published on Web 11/16/2001

found structures being isostructural with the long known Co(im)$_2$ and Zn(im)$_2$ species.[15] In the latter compounds—and in the bis(4-azabenzimidazolato)iron(II) and -cobalt(II) analogues[10]—the metal atoms are nearly tetrahedral, while heavily distorted square-planar chromophores have been found in all structurally characterized Cu(im)$_2$ polymorphs. Thus, aiming at the synthesis of M(im)$_2$ species containing rigorously square-planar MN$_4$ systems, we resorted to the well-known tendency of group 10 metal ions (in their +2 oxidation state) to afford local D_{4h} symmetry. Therefore we report, in the following, on the preparation and characterization, by chemical, spectroscopic, and thermal methods, of these species and on the discovery of new interesting structural features of some intermediates in their formation by ab initio X-ray powder diffraction (XRPD) methods, which allowed the complete characterization of polymeric Ni(Him)$_2$(im)(CH$_3$COO) and of the hydrogen-bonded polymers of general M(Him)$_2$(im)$_2$ formula (M = Pd, Pt; Him = imidazole).

Noteworthy, for a variety of noble metals (including copper, gold, and platinum), electrosorption of imidazole is known to form efficient corrosion inhibitors,[16] which have been used extensively in the printed circuit board industries.[17] Thus, the studies reported in this paper may be of broader significance and lead to a "structural" interpretation of the electrochemically generated (chemisorbed) Pt/Him films.[18]

Experimental Section

General Methods. Imidazole (Him) and metal salts were used as supplied (Aldrich Chemical Co.). Solvents were purified by standard methods. Infrared spectra were recorded on a Bio-Rad FTIR 7 instrument. Thermogravimetric analyses were performed on a Perkin-Elmer TGA 7 system. DSC traces were obtained with the aid of a Perkin-Elmer DSC 7 calorimeter. Elemental analyses (C, H, N) were carried out at the Microanalytical Laboratory of the University of Milan.

Synthesis of [Ni(Him)$_2$(im)(CH$_3$COO)], 1. To a solution of Ni(CH$_3$COO)$_2$ (0.500 g, 2.83 mmol) in *n*-butanol (20 mL) was added imidazole (1.2 g, 17.6 mmol) under stirring. The blue solution was heated at 130 °C for 4 h. During this time a pale-violet solid formed. The solid was filtered off, washed with hot *n*-butanol (20 mL) and methanol (10 mL), and then dried under vacuum. Yield: 0.644 g, 71%. Anal. Calcd for C$_{11}$H$_{14}$N$_6$NiO$_6$: C, 41.16; H, 4.37; N, 26.19. Found: C, 41.22; H, 4.35; N, 25.79.

Synthesis of Ni(im)$_2$, 2-Ni (Amorphous Phase). Method a. Complex **1** (0.500 g, 1.56 mmol) was suspended in *n*-butanol (50 mL) and heated at 130 °C for 4 h. The color of the solid changed from violet to yellow. The solid was then filtered off, washed with methanol, and dried under vacuum. Yield: 0.235 g, 78%.

Method b. Complex **1** (0.300 g) was placed in a sublimation apparatus and heated at 200 °C by means of a heat gun, controlling the temperature (±5 °C) by employing a standard thermocouple. Free imidazole and CH$_3$COOH were detected on the coldfinger of the apparatus. Heating was stopped after 30 min. The solid (yellow in color) was allowed to cool and then removed, washed with methanol, and dried under vacuum. Yield: 0.153 g, 85%. IR bands (cm^{-1}): 3128 w, 1239 w, 1088 m, 826 w, 748 w, 669 w. Repeated preparations afforded elemental analyses consistent for a C$_6$H$_6$N$_4$Ni formulation (vide infra), thus suggesting, in all cases, sample purity.

Synthesis of Ni(im)$_2$, 2-Ni′ (Polycrystalline Phase). To a solution of NiCl$_2$·6H$_2$O (0.50 g, 2.10 mmol) in water (20 mL) was added imidazole (1.00 g, 14.7 mmol) under stirring. A lavender colored precipitate of [Ni(Him)$_6$]Cl$_2$ suddenly formed. Aqueous NH$_3$ (25% w/w) was added until a clear deep-blue solution formed. The solution was then refluxed for 1 h allowing the gradual formation of the solid yellow Ni(im)$_2$. The solid was then filtered out, washed with water, and dried under vacuum. Yield: 0.275 g, 68%. Anal. Calcd for C$_6$H$_6$N$_4$Ni: C, 37.36; H, 3.11; N, 29.06. Found: C, 36.94; H, 2.98; N, 28.81.

Synthesis of Pd(Him)$_2$(im)$_2$, 3-Pd. To a solution of K$_2$PdCl$_4$ (1.00 g, 3.06 mmol) in water (25 mL) was added imidazole (1.04 g, 15.3 mmol). A small amount of a white-colored precipitate of [Pd(Him)$_4$]Cl$_2$[19] gradually formed while the color of the dissolved K$_2$PdCl$_4$ faded. After 2 h of stirring, Et$_3$N (0.85 mL, 6.13 mmol) was added dropwise, resulting in a conspicuous precipitation of a white solid. The suspension was stirred for an additional 1 h, and the solid was then filtered out, washed with water, and dried under vacuum. Yield: 1.09 g, 95%. Anal. Calcd for C$_{12}$H$_{14}$N$_8$Pd: C, 38.26; H, 3.72; N, 29.76. Found: C, 38.15; H, 3.68; N, 29.82.

Synthesis of Pt(Him)$_2$(im)$_2$, 3-Pt. The synthesis of this species has already been reported, but unexpectedly, the authors could not prepare the Pd species analogue by the same synthetic route.[19] On the contrary, complex **3-Pt** was obtained starting from K$_2$PtCl$_4$ by employing the same synthetic procedure used for complex **3-Pd**. Yield: 97%. Anal. Calcd for C$_{12}$H$_{14}$N$_8$Pt: C, 30.97; H, 3.01; N, 24.09. Found: C, 30.01; H, 2.89; N, 23.78.

Synthesis of {Pd$_{0.5}$Pt$_{0.5}$}(Him)$_2$(im)$_2$, 3-Pd/Pt. The bimetallic derivative **3-Pd/Pt** was obtained employing the same synthetic procedure used for complex **3-Pd** starting from a solution containing equimolar amounts of K$_2$PdCl$_4$ and K$_2$PtCl$_4$. Yield: 97%. Anal. Calcd for C$_{24}$H$_{28}$N$_{16}$PdPt: C, 34.23; H, 3.33; N, 26.62. Found: C, 34.11; H, 3.37; N, 26.19.

Synthesis of Pd(im)$_2$, 2-Pd. In a typical preparation, the homoleptic derivative **2-Pd** was obtained by suspending 500 mg (1.33 mmol) of complex **3-Pd** in water and heating at 70 °C for 2 h. The solid was then filtered out, washed with hot water and methanol, and dried under vacuum. Yield: 0.313 g, 98%. Anal. Calcd for C$_6$H$_6$N$_4$Pd: C, 29.95; H, 2.50; N, 23.29. Found: C, 30.01; H, 2.52; N, 23.08. IR bands (cm^{-1}): 3122 w, 1239 w, 1088 m, 821 w, 740 w, 665 w.

Synthesis of Pt(im)$_2$, 2-Pt. Pt(im)$_2$ was obtained in a similar manner by starting from Pt(Him)$_2$(im)$_2$, **3-Pt**. Yield: 98%. Anal. Calcd for C$_6$H$_6$N$_4$Pt: C, 21.88; H, 1.82; N, 17.02. Found: C, 21.66; H, 1.57; N, 16.89. IR bands (cm^{-1}): 3126 w, 1239 w, 1089 m, 819 w, 740 w, 667 w.

X-ray Powder Diffraction Analysis of 1, 3-Pd, and 3-Pt. The gently ground powders were cautiously deposited in the hollow of an aluminum holder equipped with a zero background plate (supplied by The Gem Dugout, State College, PA). Diffraction data (Cu Kα, λ = 1.5418 Å) were collected on a vertical scan PW1820 diffractometer, equipped with parallel (Soller) slits, a secondary beam curved graphite monochromator, a Na(Tl)I scintillation detector, and pulse height amplifier discrimination. The generator was operated at 40 kV and 40 mA. Slits used: divergence 1.0°; antiscatter 1.0°; receiving 0.2 mm. Nominal resolution for the present setup is 0.14° in 2θ (fwhm) for the Si(111) peak at 28.44° (2θ). Long overnight scans were performed with $5 < 2\theta < 105°$, t = 10 s, and $\Delta 2\theta = 0.02°$.

Indexing, using TREOR,[20] of the low-angle diffraction peaks suggested a primitive orthorhombic cell of approximate dimensions a = 16.91, b = 14.92, and c = 5.55 Å for **3-Pd** [$M(18)$[21] = 16; $F(18)$[22] = 23 (0.012, 67)] and primitive monoclinic cells a = 12.37, b = 14.88, and c = 8.67 Å and β = 112.8° [$M(18)$ = 25; $F(18)$ = 47 (0.009, 43)] and a = 5.34, b = 15.65, and c = 8.65 Å and β = 103.3° [$M(18)$ = 16; $F(18)$ = 24 (0.017, 45)] for **1** and **3-Pt**, respectively. Systematic absences for **1, 3-Pd**, and **3-Pt** indicated $P2_1/a$, $Pnca$, and $P2_1/c$,

(15) Sturm, M.; Nrandel, F.; Engel, D.; Hoppe, W. *Acta Crystallogr.* **1976**, *B31*, 2369. Lehnert, R.; Seel, F. *Z. Anorg. Allg. Chem.* **1980**, *464*, 187.
(16) Xue, G.; Jiang, S.; Huang, X.; Shi, G.; Sun, B. *J. Chem. Soc., Dalton Trans.* **1988**, 1487. Xue, G.; Dai, Q.; Jiang, S. *J. Am. Chem. Soc.* **1988**, *110*, 2393. Gašparac, R.; Martin, C. R.; Stupnišek-Lisac, E.; Mandic, Z. *J. Electrochem. Soc.* **2000**, *147*, 991 and references therein.
(17) See for example: Katnani, A. D.; Papathomas, K. I.; Drolet, D. P.; Lees, A. J. *J. Therm. Anal.* **1989**, *35*, 147 and references therein.
(18) Pekmez, K.; Yildiz, A. *Z. Phys. Chem.* **1996**, *196*, 109.
(19) Van Kralingen, C. G.; De Ridder, J. K.; Reedijk, J. *Inorg. Chim. Acta* **1979**, *36*, 69.
(20) Werner, P. E.; Eriksson, L.; Westdahl, M. *J. Appl. Crystallogr.* **1985**, *18*, 367.
(21) De Wolff, P. M. *J. Appl. Crystallogr.* **1968**, *1*, 108.
(22) Smith, G. S.; Snyder, R. L. *J. Appl. Crystallogr.* **1979**, *12*, 60.

Table 1. Crystal Data and Refinement Parameters for Compounds $Ni(Him)_2(im)(CH_3COO)$, **1**, $Pd(Him)_2(im)_2$, **3-Pd**, and $Pt(Him)_2(im)_2$, **3-Pt**

	1	**3-Pd**	**3-Pt**
species	$Ni(Him)_2(im)(CH_3COO)$	$Pd(Him)_2(im)_2$	$Pt(Him)_2(im)_2$
formula	$C_{11}H_{14}N_6NiO_2$	$C_{12}H_{14}N_8Pd$	$C_{12}H_{14}N_8Pt$
fw	320.98	376.70	465.35
cryst system	monoclinic	orthorhombic	monoclinic
space group	$P2_1/a$	*Pnca*	$P2_1/c$
a, Å	12.3467(7)	16.930(1)	5.3403(3)
b, Å	14.8671(8)	14.934(1)	15.680(1)
c, Å	8.6676(6)	5.5583(3)	8.6655(5)
α, deg	90	90	90
β, deg	112.788(5)	90	103.354(4)
γ, deg	90	90	90
V, Å^3	1466.8(2)	1405.4(1)	705.17(7)
Z	4	4	2
ρ_{calc}, g cm^{-3}	1.453	1.783	2.186
μ(Cu Kα), cm^{-1}	19.8	109.9	188.3
diffractometer	Philips PW1820	Philips PW1820	Philips PW1820
T, K	298	298	298
2*θ* range, deg	10−90	10−100	8−105
N_{obs}	4001	4501	4750
N_{refl}	1178	717	783
R_{wp}, R_p[a]	0.155, 0.110	0.067, 0.052	0.088, 0.063
R_F[a]	0.081	0.064	0.038

[a] $R_p = \sum|y_{i,o} - y_{i,c}|/\sum y_{i,o}$; $R_{wp} = [\sum w_i(y_{i,o} - y_{i,c})^2/\sum w_i y_{i,o}^2]^{1/2}$; $R_F = \sum|F_{k,o}\text{-}F_{k,c}|/\sum F_{k,o}$, where y_i and F_k are the (observed and calculated) profile intensities and structure factors, respectively, w_i is a statistical weighting factor, taken as $1/y_{i,o}$, and *i* runs over all *N* data points and *k* over the space group permitted reflections. Due to the extensive use of geometrical restraints, χ^2 values of statistical significance are not available.

respectively, as the probable space groups, later confirmed by successful solution and refinement. Structure solutions were initiated by using EXPO,[23] which afforded the location of the metal atoms and those of a few nitrogen atoms bound to them. Difference Fourier syntheses and geometrical modeling later afforded approximate coordinates for the remaining non-hydrogen atoms.

The final refinements were performed with the aid of the GSAS suite of programs,[24] by imposing geometric constraints to chemically stiff imidazolate rings (C−C and C−N were given average literature values of 1.38 Å, and internal ring angles were fixed at 108°). Soft restraints were also applied to M−N [2.1(2) Å] and M−O distances [2.2(2) Å]. The peak shapes were best described by the Thompson/Cox/Hastings formulation[25] of the pseudo-Voigt function, with GV and LY set to zero. The background functions were described by a cosine Fourier series, while systematic errors were corrected with the aid of a sample-displacement angular shift; a single (refinable) isotropic displacement parameter [U_{iso}(M)] was assigned to Ni, Pd, or Pt, while lighter atoms *U*'s were arbitrarily given [U_{iso}(M) + 0.02] Å^2 values. The contribution of the hydrogen atoms to the scattered intensity was neglected. Scattering factors, corrected for real and imaginary anomalous dispersion terms, were taken from the internal library of GSAS. Final R_p, R_{wp}, and R_F agreement factors, together with details of the data collections and analyses for the three crystal phases, can be found in Table 1. Figure 1 shows the final Rietveld refinement plots for **1**, **3-Pd,** and **3-Pt**, respectively. Final fractional coordinates and full lists of bond distances and angles are supplied as Supporting Information.

The structure of the mixed-metal phase, **3-Pd/Pt**, obtained by simultaneous precipitation of a 1:1 mixture of Pd and Pt complexes has also been refined, using an additional free site occupancy factor for the platinum atom, estimated as 0.805(9), corresponding to a $Pd_{0.48(2)}$-$Pt_{0.52(2)}$ formulation.

Results and Discussion

The main goal of the synthetic work was to obtain analytically pure products in a crystalline, *although powdered*, form, suitable for an XRPD analysis and, therefrom, for their complete structural determination.

Synthesis of the Nickel Derivatives. In the past, two synthetic routes leading to $Ni(im)_2$ have been reported: (i) treatment of nickel(II) salts with excess imidazole in the presence of bases[26]

$$NiX_2 + 2Him \rightarrow Ni(im)_2 + 2X^- \quad X = Cl, NO_3 \qquad (1)$$

and (ii) thermal decomposition of the $[Ni(acac)_2(Him)_2]$ derivative[27]

$$[Ni(acac)_2(Him)_2] \xrightarrow{260\ ^\circ C} Ni(im)_2 + 2Hacac \qquad (2)$$

Both strategies afford analytically pure, but completely amorphous, $Ni(im)_2$ powders. In the search of alternative synthetic paths, we initially employed Ni(II) acetate as a starting material. When a solution of $Ni(CH_3COO)_2$ was refluxed in the presence of excess Him in *n*-butanol, the formation of a pale violet derivative analyzing as $Ni(Him)_2(im)(CH_3COO)$, **1**, was observed.

Complex **1** derives from the partial deprotonation of the imidazoles bound to the metal ions,[28] forced by the weakly basic nature of the acetate ions (eq 3). The IR spectrum of **1** well matches the given formulation, showing a broad absorption at about 3300 cm^{-1} (due to the neutral imidazole ligands) and three bands in the 1550−1600 cm^{-1} region, attributable to the so-called ring breathing of the neutral and anionic heterocyclic rings and to the υ_{as}(COO) stretching. The full crystallographic characterization of **1** was performed by means of XRPD (see below), revealing the polymeric nature of this species:

(23) Altomare, A.; Burla, M. C.; Cascarano, G.; Giacovazzo, C.; Guagliardi, A.; Moliterni, A. G. G.; Polidori, G. *J. Appl Crystallogr.* **1995**, *28*, 842.
(24) Larson, A. C.; Von Dreele, R. B. *LANSCE, MS-H805*; Los Alamos National Laboratory: Los Alamos, NM, 1990.
(25) Thompson, P.; Cox, D. E.; Hastings, J. B. *J. Appl. Crystallogr.* **1987**, *20*, 79.
(26) Bauman, J. E.; Wang, J. C. *Inorg. Chem.* **1964**, *3*, 368.
(27) Döring, M.; Ludwig, W.; Meinert, M.; Uhlig, E. *Z. Anorg. Allg. Chem.* **1991**, *595*, 45.
(28) Probably, in the neutral complex $Ni(Him)_4(CH_3COO)_2$, recently reported in the following: Naumov, P.; Ristova, M.; Drew, M. G. B.; Ng, S. W. *Acta Crystallogr.* **2000**, *C56*, 372.

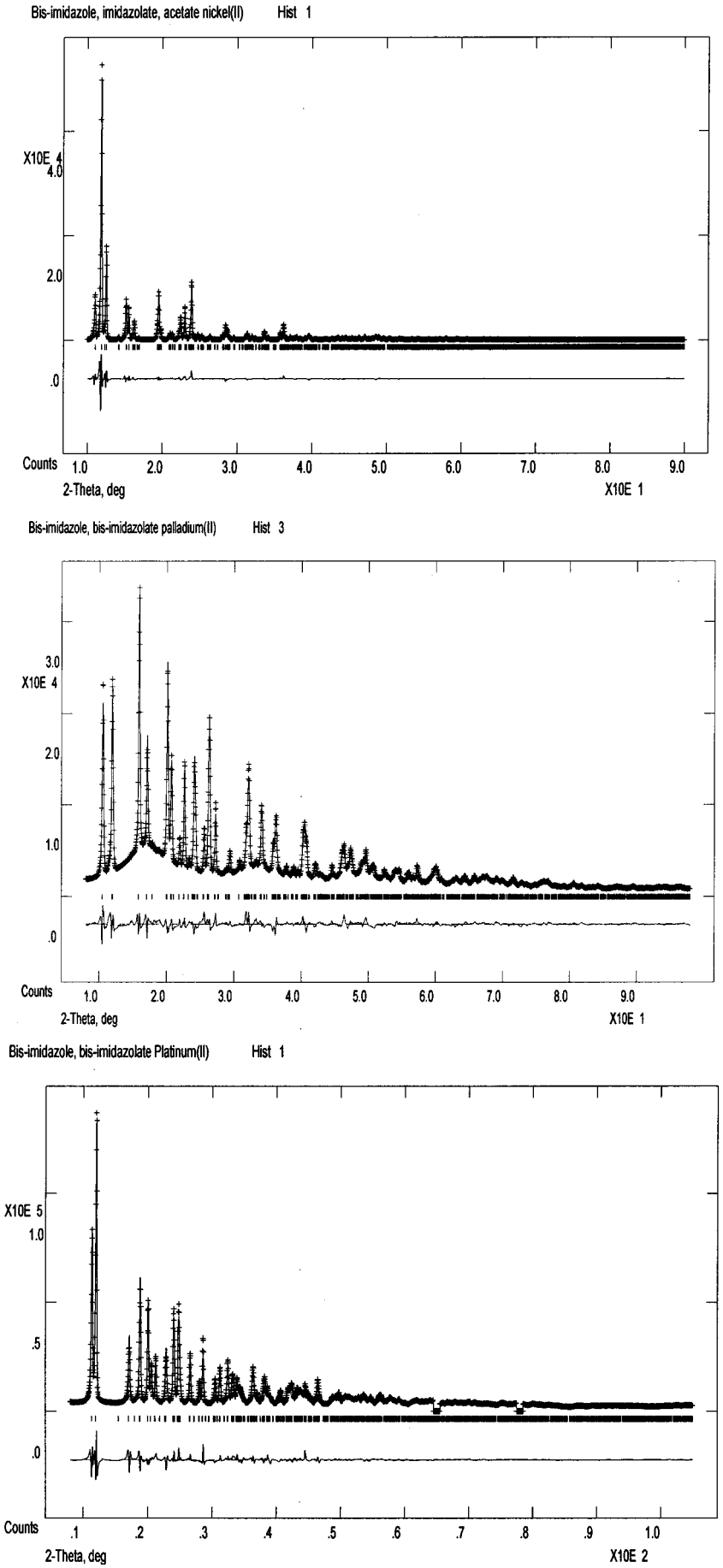

Figure 1. Top to bottom: Rietveld refinement plots for **1**, **3-Pd**, and **3-Pt**, with difference plots and peak markers. The two small regions excluded from the final refinement of **3-Pt** contain spurious peaks from the sample holder.

$$Ni(CH_3COO)_2 + 3Him \rightarrow Ni(Him)_2(im)(CH_3COO) + CH_3COOH \quad (3)$$

By the reflux of complex **1** in *n*-butanol in the absence of free imidazole, a further elimination reaction takes place and the quantitative formation of the yellow $Ni(im)_2$ species is observed:

$$Ni(Him)_2(im)(CH_3COO) \rightarrow Ni(im)_2 + CH_3COOH + Him \quad (4)$$

The same behavior was observed by heating complex **1** in the solid state, under vacuum, at 200 °C. Unfortunately, all the $Ni(im)_2$ samples obtained by this routes and by minor modifications of the conditions reported above (*T*, solvent, concentrations) showed the absence of significant peaks in the XRPD traces, thus preventing any further structural study.

However, a considerable improvement was achieved by reconsidering $NiCl_2$ as the starting material and slightly modifying the Bauman and Wang (eq 1) synthetic route.[26] $NiCl_2$ reacts in water with Him (Ni/Him ratio 1/7), giving place to the insoluble lavender colored $[Ni(Him)_6]Cl_2$ derivative.[29] While the addition to the reaction medium of a strong base as NaOH causes the sudden formation the amorphous $Ni(im)_2$ derivative,[26] when aqueous NH_3 is added at room temperature, the initial $[Ni(Him)_6]Cl_2$ species gradually dissolves, probably giving place to a complex mixture of $[Ni(NH_3)_x(Him)_{6-x}]Cl_2$ derivatives (deep blue solution). Upon heating of this solution (to reflux), the formation of a yellow precipitate of $Ni(im)_2$ was eventually observed. The yellow powders show a rich XRPD trace, which can be interpreted as a superimposition of the patterns of a polycrystalline phase, **2-Ni′**, isomorphous with the pink polymorph of $Cu(im)_2$,[14] and of a (still unknown) contaminant.

Synthesis of the Palladium and Platinum Derivatives. When reacted with imidazole, palladium and platinum behave very similarly to each other. Indeed, when imidazole is added to aqueous solutions of K_2MCl_4 (M = Pd or Pt; metal/imidazole ratio 1/5), the insoluble $[M(Him)_4]Cl_2$ derivatives initially form. The addition of Et_3N (M/amine 1/2 ratio) promotes the deprotonation of imidazole molecules and the formation of the (insoluble) imidazole/imidazolate $M(Him)_2(im)_2$ species (M = Pd, **3-Pd**; M = Pt, **3-Pt**).

$$K_2MCl_4 + 4Him \rightarrow [M(Him)_4]Cl_2 \xrightarrow{Et_3N} M(Him)_2(im)_2 \quad (5)$$

The synthesis of the platinum $Pt(Him)_2(im)_2$ species, **3-Pt**, has already been described in the literature.[19] However, in the same paper, the absence of reactivity of K_2PdCl_4 with Him was outlined. Differently from what reported therein, we have not perceived any substantial difference in the reactivity of the palladium and platinum salts, as demonstrated by the facile isolation of both species **3-Pd** and **3-Pt**.

The IR spectra of complexes **3-Pd** and **3-Pt** are very similar. The most striking feature is the presence of broad bands centered at 2060 and 2500 cm^{-1} in **3-Pd** and 1927 and 2500 cm^{-1} in **3-Pt**. It is well-known that these absorption bands are imputable to strong hydrogen bonds and are frequently found in complexes containing both pyrazole and pyrazolate ligands,[30] such as the strictly related $[Pd(Hdmpz)_2(dmpz)_2]_2$ or $[Pt(Hpz)_2(pz)_2]_2$ derivatives (Hdmpz = 3,5-dimethylpyrazole, Hpz = pyrazole). However, differently from these *dimeric* species, the XRPD structural analysis revealed the *polymeric* nature of complexes **3-Pd** and **3-Pt**, based on the juxtaposition of H-bonded $M(Him)_2(im)_2$ units and the different steric requirements of imidazole with respect to pyrazole (see later).

Despite these strong hydrogen bonds, the neutral imidazole molecules can be easily removed from **3-Pd** and **3-Pt** by heating the complexes in the solid state under vacuum or suspending them in hot water. The formation of the (analytically pure) *binary* $M(im)_2$ species (M = Pd, **2-Pd**; M = Pt, **2-Pt**) is in both cases observed:

$$M(Him)_2(im)_2 \rightarrow M(im)_2 + 2Him \quad (6)$$

Complexes **2-Pd** and **2-Pt** showed quite identical IR spectra (see Experimental Section), indicative of a similar molecular structure. Unfortunately, all samples obtained by this way (and by slight modifications of this synthetic approach) exhibited XRPD traces containing only amorphous peaks, precluding, again, a detailed structural study. Needless to say, work is in due course with the aim to obtain microcrystalline samples.

Thermal Behavior. When heated under nitrogen, $Ni(Him)_2(im)(CH_3COO)$ loses, below 200 °C, acetic acid and imidazole, affording amorphous $Ni(im)_2$, which is found to be thermally stable up to ca. 420 °C, where decomposition to metallic nickel and elimination of the organic part occur. Parallel XRPD and DSC measurements showed that such amorphous yellow powders of $Ni(im)_2$ do not convert, upon heating, into a stable crystalline phase. Thus, this species behaves rather differently from the *amorphous* $Ni(pymo)_2$ congener (Hpymo = 2-hydroxypyrimidine), which was found to transform, near 315 °C, into a microcrystalline powder, stable up to ca. 550 °C.[31]

When heated under nitrogen, $Pd(Him)_2(im)_2$, **3-Pd**, loses imidazole (endotherm near 150 °C) and affords amorphous $Pd(im)_2$, **2-Pd**, which is stable up to ca. 400 °C, Pd metal being recovered at higher temperatures. Of higher thermal stability, $Pt(Him)_2(im)_2$, **3-Pt**, generates $Pt(im)_2$, **2-Pt**, at ca. 250 °C, which decomposes to Pt metal only above 450 °C. The DSC and TGA traces of the mixed-metal phase **3-Pd/Pt**, $(Pd_{0.5}Pt_{0.5})(Him)_2(im)_2$, manifest an intermediate behavior, the two events occurring near 190 and 440 °C. Inter alia, these observations exclude the copresence of two isomorphous, but segregated, Pd/Pt phases, giving "almost superimposable" XRPD patterns (see below).

Crystal Structure of $Ni(Him)_2(im)(CH_3COO)$, 1. Crystals of this species contain octahedrally coordinated nickel(II) ions, each bound to two monodentate Him ligands, one chelating acetate fragment and two nitrogen atoms (trans to each other) from distinct imidazolate fragments (see Figure 2a). Each im anion bridges, in the common exobidentate fashion, metal atoms which are related by the *a* glide symmetry operation, thus generating, within the crystal, one-dimensional polymeric chains, running parallel to *a*, built upon a Ni−(μ-im)−Ni− backbone, and branched, at the nickel atoms, by two Him and one acetate ligands. The overall packing of these chains, in the *bc* plane, is

(29) (a) Goodgame, D. M. L.; Goodgame, M.; Hayward, P. J.; Rayner-Canham G. W. *Inorg. Chem.* **1968**, *7*, 2447. (b) Eilbeck, W. J.; Holmes, F.; Underhill, A. E. *J. Chem. Soc.* **1967**, 757. Jansen, J. C.; Reedijk, J. *Z. Naturforsch., B* **1974**, *29*, 527.

(30) See for example: (a) Ardizzoia, G. A.; La Monica, G.; Cenini, S.; Moret, M.; Masciocchi, N. *J. Chem. Soc., Dalton Trans.* **1996**, 1351. (b) Masciocchi, N.; Ardizzoia, G. A.; LaMonica, G.; Moret, M.; Sironi, A. *Inorg. Chem.* **1997**, *36*, 449. (c) Burger, W.; Strähle, J. Z. *Z. Anorg. Allg. Chem*. **1986**, *539*, 27. Carmona, D.; Oro, L. A.; Lamala, M. P.; Elguero, J.; Apreda, M. C.; Foces-Foces, C.; Cano, F. H. *Angew. Chem., Int. Ed. Engl.* **1986**, *25*, 1114.

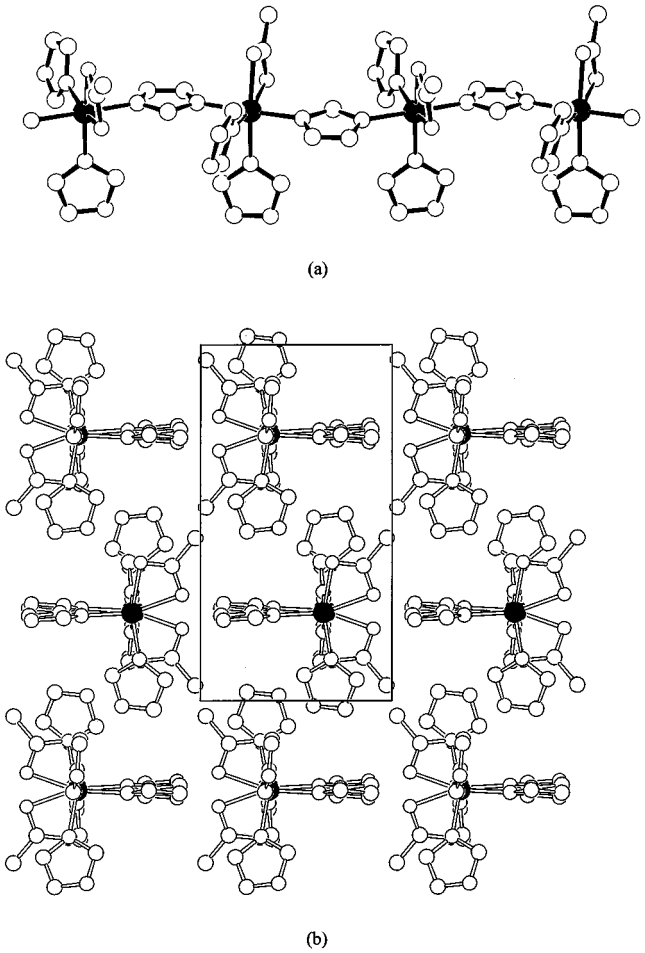

Figure 2. (a) Drawing of a portion of the polymeric $[Ni(Him)_2(CH_3COO)(im)]_n$ chain, generated by the *a*-glide symmetry operation. Ni atoms are in black, and H atoms are not shown. (b) Pseudohexagonal packing of the chains, viewed down *a*.

pseudohexagonal (see Figure 2b) and is further stabilized by hydrogen bonds connecting N−H residues of the "equatorial" imidazoles with oxygen atoms of the acetates of neighboring chains (N···O = 2.66−2.79 Å). Thus, considering this system of hydrogen-bonded interactions, a supramolecular 3D assembly can be envisaged, which the rather poor solubility of this species can be possibly assigned to. The refined Ni···Ni distance, of ca. 6.17 Å (*a*/2), appears to be among the longest μ_2,η^1,η^1-imidazolate-bridged metal−metal interactions; for example, for first-row transition metals, this value falls in the 5.73−6.1 Å range, with the notable exception of the 6.14−6.20 Å values found in $Fe_3(im)_6(Him)_3$.[32] The overall structure bears clear resemblance to that of $Cu(im)(Him)_2Cl$,[33] which, although containing pentacoordinated metal atoms, also shows large Cu···Cu distances within infinite $[Cu-(\mu\text{-im})-]_n$ (psudohexagonally packed) chains, "radial" imidazoles, and monoanionic ligands (in this case, Cl^- ions), mutually interacting through intermolecular hydrogen bonds (N−H···Cl = 3.22 Å). Most distinctively, owing to the relative orientations of the ligands, the overall packings in these related species are centrosymmetric in $Ni(Him)_2(im)(CH_3COO)$ and acentric (and polar) in $Cu(im)(Him)_2Cl$.

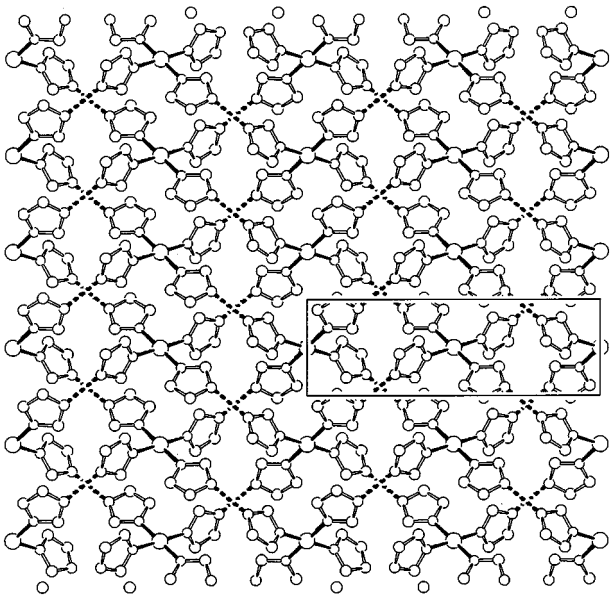

Figure 3. Drawing of a portion of the polymeric $Pd(Him)_2(im)_2$ species, viewed down [010] (vertical axis = *c*). H atoms are not shown. Fragmented bonds refer to H-bonded N···N contacts (see text). Note the entanglement of two distinct 2D frameworks of pseudosquare meshes.

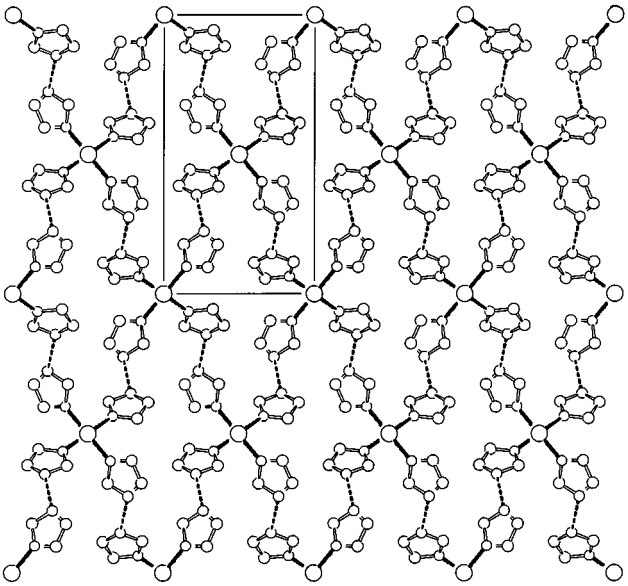

Figure 4. Drawing of a portion of the polymeric $Pt(Him)_2(im)_2$ species, viewed down [100] (vertical axis = *b*). H atoms are not shown. Fragmented bonds refer to H-bonded N···N contacts (see text).

Crystal Structures of $M(Him)_2(im)_2$ (M = Pd, 3-Pd; M = Pt, 3-Pt). Although long known,[19] the $Pt(Him)_2(im)_2$ species, in the absence of single crystals of suitable size and quality, remained until now structurally uncharacterized; however, a timid formulation as a dimeric molecule has appeared (mostly based on analogies with the $[Pt(pz)_2(Hpz)_2]_2$ congener and on weak spectroscopic evidences[30c]). Our powder diffraction work has demonstrated that crystals of these (*nonisomorphous*) $M(Him)_2(im)_2$ species contain square planar M atoms, located, in both cases, onto crystallographic inversion centers (see Figures 3 and 4). Of the four nitrogen atoms bound to each metal, two can be formally assigned to neutral Him ligands and the remaining two to monodentate im fragments. However, since, in both cases, rather evident hydrogen bonds (N−H···N

(31) Masciocchi, N.; Ardizzoia, G. A.; La Monica, G.; Maspero, A.; Sironi, A. *Eur. J. Inorg.Chem.* **2000**, 2507.
(32) Rettig, S. J.; Storr, A.; Summers, D. A.; Thompson, R. C.; Trotter, J. *J. Am. Chem. Soc.* **1997**, *119*, 8675.
(33) Lundberg, B. K. S. *Acta Chem. Scand.* **1972**, *26*, 3902.

ca. 2.75 Å, already postulated in ref 19) occur between Him and im fragments bound to *different* metal atoms which are nearly 10 Å apart, this distinction fails, and a *single* (hydrogen-bonded) ligand, i.e. [im-H-im], bridging these long metal−metal interactions can be idealized. Formally, this would parallel the well-known structural features of the $[XHX]^-$ anions (X = F, OH[34]), although we cannot foresee, on the basis of our diffraction and spectroscopic data alone, whether the bridging H atom lies within a single- or double-well potential. A very similar situation can be found in purely organic pyrazoles[35] (cyclic or polymeric catamers) and in the $[M(Hpz)_2(pz)_2]_2$ and $[M(Hdmpz)_2(dmpz)_2]_2$ analogues (M = Pd, Pt; Hdmpz = 3,5-dimethylpyrazole), in their different crystal phases.[30c,36] Thus, idealizing [im-H-im] as a single ligand, it can be assigned stereochemical features similar to other simpler fragments of this class, such as pyrazolate, imidazolate, and pyrimidin-2-olate, all of which can act as exobidentate, monoanionic bridging ligands. However, the flexibility of the im-H-im torsional angle should grant, in this case, much higher structural versatility than for all cited stiff heterocycles. Consistently, a cisoid im-H-im link (about the N···N hinge) is observed in the palladium derivative (ca. 44°, measured by the *a*−*b*−*c*−*d* torsion of the $(Pd)N_a-N_b\cdots N_c-N_d(Pd)$ fragment), while a transoid conformation occurs in the platinum complex (ca. 124°). A similar stereochemical analysis, necessary for the interpretation of the structural features of cyclic oligomers and of linear polymers of the M(pz*) phases (M = Cu, Ag, Au; Hpz* = a generic 3,5-substituted pyrazole), has already been presented and associated with the linear, *but flexible*, pz*−M−pz* link.[12a] For the sake of completeness, upon using this "nomenclature", in all known $M(pz^*)_2(Hpz^*)_2$ phases nonbonding M···M interactions (of ca. 3.7 Å) are quadruply bridged by pz*−H−pz* links of the cis type.

Upon considering the overall connectivity of the metal-to-metal links (through this new im−H−im ligand), in both species layers of (pseudo)square meshes (running normal to [010] and [100] in **3-Pd** and **3-Pt**, respectively) can be observed, which, in the case of Pt, are clearly distinct, while, in the Pd derivative, form an entangled structure based upon interpenetrating 2D layers, coupled in pairs. As anticipated in the Experimental Section, when a 1:1 mixture of Pd/Pt complexes is reacted with imidazole and Et_3N, a monophasic powder is obtained [isomorphous with $Pt(Him)_2(im)_2$] which contains statistically disordered metal atoms (XRPD evidence). Moreover, to force the preparation of a still unknown, pure $Pd(Him)_2(im)_2$ phase, ***β*-3-Pd**, isomorphous with **3-Pt**, we have prepared the palladium derivative in the presence of a minor amount (less than 5%) of solid **3-Pt**. Unfortunately, the resulting mixture contained **3-Pd** contaminated by **3-Pt**, thus showing that the latter had not driven crystallization toward ***β*-3-Pd**. As a further effort, we have also tried to induce nucleation of the purported ***β*-3-Pd** phase by employing traces of suspended **3-Pt** during the preparation of $Pd(im)_2(Him)_2$; also in this case, only **3-Pd** was recovered.

Conclusions

That the imidazole/imidazolate Pd and Pt derivatives sharing the same formula are not isostructural nor, obviously, isomorphous, is somewhat a surprise; indeed, electronic and steric effects are expected to be very similar in both metals and, therefore, to similarly influence the nature of their "parallel" species. Presently, we have no sound explanation for the existence of the two structurally distinct phases discussed above, unless subtle kinetic effects during crystal nucleation (i.e. polymer formation) are at work (as invoked for the different reactivity of isostructural Pd/Pt macrocycles[37]); noteworthy, also the $Pt(Bim)_4X_2$ species (Bim = benzimidazole and X = Cl, Br, NO_2, NCS[38]), the Pd analogues of which are easily prepared, have never been isolated, all efforts ending up in the formation of the diacido $Pt(Bim)_2X_2$ complexes. However, it should be noted that polymeric, and even molecular, species of this class are known to afford, depending on the actual conditions employed, different crystal phases (polymorphs)[14] or cyclic oligomers (and one-dimensional chain polymers) of different nuclearity.[12] Thus, a disentangled form of $Pd(Him)_2(im)_2$ (***β*-3-Pd**) and, conversely, interpenetration of 2D layers in $Pt(Him)_2(im)_2$ may be occasionally discovered in the future, if suitable conditions (concentration, temperature, solvent polarity and viscosity, and rates of reaction and of the workup) are encountered. Accordingly, the occurrence of a monophasic 1:1 mixed metal species speaks for the (still theoretical) accessibility of ***β*-3-Pd**, a $Pd(Him)_2(im)_2$ phase isomorphous with $Pt(Him)_2(im)_2$.

In addition, we have proved that, differently from their cobalt, copper, and zinc analogues,[14,15] $M(im)_2$ species (M = Ni, Pd, and Pt) are very prone to afford amorphous structures, with the notable exception of the polycrystalline $Ni(im)_2$, **2-Ni′**, crystallized from hot solutions, which appears to be isomorphous with the *pink* $Cu(im)_2$ phase.[14] Unfortunately, the structural motif of the latter is still unknown, nor could it be derived from the complex pattern of **2-Ni′**, which contains an unknown contaminant polycrystalline phase—possibly another polymorph. Nevertheless, the structural chemistry of Ni(II), its bright yellow color (identical with that of $Ni(pz)_2$, which contains square-planar NiN_4 chromophores[39]), and the structure−properties correlations put forward in ref 14 for *pink* $Cu(im)_2$, strongly suggest, for all these species, a local D_{4h} coordination mode. In addition, the strict similarity of the IR absorption pattern for the three amorphous $M(im)_2$ species (M = Ni, Pd, Pt) also speaks for similar local coordination geometries, which, for Pd and Pt, are undoubtedly square-planar. Work is in progress to obtain monophasic polycrystalline samples and XRPD data of sufficient quality for their full ab initio structure determination.

Acknowledgment. We thank the Italian Consiglio Nazionale delle Ricerche (CNR) and MURST for funding. We also acknowledge financial support from ICDD, International Centre for Diffraction Data (Grant-in-Aid Program 1999−2000).

Supporting Information Available: Full listings of fractional atomic coordinates and bond distances and angles for compounds **1**, **3-Pd**, and **3-Pt**. This material is available free of charge via the Internet at http://pubs.acs.org.

IC010585D

(34) Cotton, F. A.; Wilkinson, G.; Murillo, C.; Bochmann, M. *Advanced Inorganic Chemistry*, 6th ed.; Wiley: New York, 1999; pp 69, 464.
(35) De Paz, J. L. G.; Elguero, J.; Foces-Foces, C.; Llamas-Saiz, A. L.; Aguilar-Parrilla, F.; Klein, O.; Limbach, H.-H. *J. Chem. Soc., Perkin Trans.* **1997**, *2*, 101. Bertolasi, V.; Gilli, P.; Ferretti, V.; Gilli, G.; Fernàndez-Castaño, C. *Acta Crystallogr.* **1999**, *B55*, 985 and references therein.
(36) Ardizzoia, G. A.; La Monica, G.; Cenini, S.; Moret, M.; Masciocchi, N. *J. Chem. Soc., Dalton Trans.* **1996**, 1351. Masciocchi, N.; Ardizzoia, G. A.; La Monica, G.; Moret, M.; Sironi, A. *Inorg. Chem.* **1997**, *36*, 449.
(37) Fujita, M.; Ogura, K. *Bull. Chem. Soc. Jpn.* **1996**, *69*, 1471.
(38) Ghosh, S. P.; Bhattacharjee, P.; Dubey, L.; Mishra, L. K. *J. Indian Chem. Soc.* **1977**, *54*, 230.
(39) Masciocchi, N.; Ardizzoia, G. A.; La Monica, G.; Maspero, A.; Sironi, A. To be published.